



Published in final edited form as:

Med Image Comput Assist Interv. 2015 October ; 9349: 117–124. doi:

10.1007/978-3-319-24553-9_15

Sparse Bayesian Inference of White Matter Fiber Orientations from Compressed Multi-resolution Diffusion MRI

Pramod Kumar Pisharady¹, Julio M Duarte-Carvajalino¹, Stamatios N Sotiropoulos², Guillermo Sapiro^{3,4}, and Christophe Lenglet¹

¹CMRR, Radiology, University of Minnesota, Minneapolis, Minnesota, USA

²FMRIB, John Radcliffe Hospital, University of Oxford, Headington, UK

³Electrical and Computer Engineering, Duke University, Durham, USA

⁴Biomedical Engineering and Computer Science, Duke University, Durham, USA

Abstract

The RubiX [1] algorithm combines high SNR characteristics of low resolution data with high spacial specificity of high resolution data, to extract microstructural tissue parameters from diffusion MRI. In this paper we focus on estimating crossing fiber orientations and introduce sparsity to the RubiX algorithm, making it suitable for reconstruction from compressed (under-sampled) data. We propose a sparse Bayesian algorithm for estimation of fiber orientations and volume fractions from compressed diffusion MRI. The data at high resolution is modeled using a parametric spherical deconvolution approach and represented using a dictionary created with the exponential decay components along different possible directions. Volume fractions of fibers along these orientations define the dictionary weights. The data at low resolution is modeled using a spatial partial volume representation. The proposed dictionary representation and sparsity priors consider the dependence between fiber orientations and the spatial redundancy in data representation. Our method exploits the sparsity of fiber orientations, therefore facilitating inference from under-sampled data. Experimental results show improved accuracy and decreased uncertainty in fiber orientation estimates. For under-sampled data, the proposed method is also shown to produce more robust estimates of fiber orientations.

Keywords

Sparse Bayesian inference; compressive sensing; linear un-mixing; diffusion MRI; fiber orientation; brain imaging

1 Introduction

Multi-compartment models [2, 3] are used to represent the diffusion MR signal from the brain white matter and to estimate microstructure features of the imaged tissue. Estimation of orientations and volume fractions of anisotropic compartments in these models helps infer the white matter fiber anatomy [4]. However accurate estimation of these parameters is challenged by the relatively limited spatial resolution of acquired diffusion MRI (dMRI) data. Advances in magnetic field strength has significantly improved spatial resolution [5,

6], although it may lead to increased noise and scanning time. Computational approach to improve the scan resolution includes the super resolution reconstruction proposed by Scherrer *et al.* [7]. One effective way to mitigate the effects of noise is the multi-resolution data fusion approach introduced in RubiX [1], which combines high SNR characteristics of low resolution (LR) data with high spatial specificity of high resolution (HR) data. This further allows combining images with different diffusion contrast at different spatial resolutions without reducing the SNR. Compressed sensing approaches [8–11] are effective ways to deal with increased scan time, which result in less measurements (diffusion directions) within a voxel.

Considering the limited number of crossing fiber bundles within a voxel, sparsity can be introduced for better and faster inference on the anisotropic compartments. In this paper, we introduce sparsity based representation and inference into the data fusion approach of RubiX, combining the benefits of regularized noise and reduced scan time. Finding volume fractions and fiber directions with a large number of possible fiber orientations is computationally expensive. We demonstrate that sparsity based approaches are useful in addressing this issue.

Without loss of generality, we represent the HR data using the ball & stick model [2, 3], in a convenient dictionary form. The volume fractions of compartments, which form the dictionary weights, are all positive and those sum to one [3]. The positivity and sum-to-one constraints, the natural constraints for fiber volume fraction estimation, make the sparse representation and inference especially challenging. We formulate the estimation of volume fractions as a linear un-mixing inference problem [12]. The volume fractions and fiber directions are estimated using a semi-supervised hierarchical Bayesian linear un-mixing approach, which is an extension of sparse Bayesian inference dealing with constraints [13, 8].

2 Methods

2.1 Dictionary Representation of High Resolution Data

The HR data is represented using a dictionary containing exponential decay component vectors in the compartment model. The measured dMRI signal at each HR voxel is first modeled using the ball & stick (1) model [2, 3].

$$S_{HR}^k = S_{HR}^0 \left[\left(1 - \sum_{n=1}^N f_n \right) e^{-b_k d} + \sum_{n=1}^N f_n e^{-b_k d (g_k^T v_n)^2} \right] \quad (1)$$

where,

S_{HR}^k the signal at HR voxel after application of k^{th} diffusion-sensitizing gradient with direction g_k and b-value b_k ,

S_{HR}^0 the HR signal without diffusion gradient applied,

f_n the volume fraction of anisotropic compartment with orientation v_n , and d the apparent diffusivity.

The measured signal at an HR voxel is the sum of the attenuation signal and measurement noise (2).

$$y_{HR}^k = \frac{S_{HR}^k}{S_{HR}^0} + \eta_{HR}^k \quad (2)$$

Based on (1) and (2), the measured signal along all K diffusion-sensitizing directions can be written in a *dictionary* form (3) as follows:

$$\mathbf{y}_{HR} = \begin{pmatrix} e^{-b_1 d} & e^{-b_1 d (g_1^T v_1)^2} & \dots & e^{-b_1 d (g_1^T v_N)^2} \\ \vdots & \vdots & \ddots & \vdots \\ e^{-b_K d} & e^{-b_K d (g_K^T v_1)^2} & \dots & e^{-b_K d (g_K^T v_N)^2} \end{pmatrix} \begin{pmatrix} f_0 \\ f_1 \\ \vdots \\ f_N \end{pmatrix} + \eta_{HR} \quad (3)$$

where,

$$f_0 = \left(1 - \sum_{n=1}^N f_n \right), f_n \geq 0.$$

Hence,

$$\mathbf{y}_{HR} = \mathbf{E}\mathbf{f} + \eta_{HR} \quad (4)$$

In equation (4), \mathbf{E} represents the local dictionary for the HR diffusion data and \mathbf{f} is the sparse representation of the HR data in this dictionary \mathbf{E} . The non-zero entries in \mathbf{f} define the number and orientation of fibers (*sticks*) in a voxel. The possible orientations of anisotropic components in the dictionary (second column onwards) are pre-specified and formed using a 5th order icosahedral tessellation of the sphere with 10242 points.

2.2 Partial Volume Representation of Low Resolution Data

In the RubiX framework, the LR data and HR data are collected from the same subject through two scans at different spatial resolutions (voxel sizes). The two datasets are aligned (if necessary) using rigid body transformations. Once the data is aligned, the LR data can be represented using corresponding HR data (data that correspond to the same physical location, but at a different spatial resolution grid), with a partial volume model [1]. The model calculates attenuation signal at an LR voxel as a linear combination of the signals at overlapping M HR voxels.

$$\frac{S_{LR}^k}{S_{LR}^0} = \sum_{m=1}^M \alpha_m \frac{S_{HR}^{km}}{S_{HR}^{0m}}, \quad \alpha_m = e^{-\frac{\|r_m - r_0\|^2}{\gamma^2}} \quad (5)$$

The HR signal contributes to the LR signal via a discretized Gaussian point spread function (PSF) with weights α_m given by the normalized Euclidean distance between the PSF center r_0 at LR voxel and the spatial position of each HR voxel r_m , and the unknown standard deviation of the PSF, γ .

2.3 Bayesian Linear Un-mixing Inference

Finding the volume fractions \mathbf{f} in (4) with a large number (N) of possible fiber orientations is an ill-posed problem. We introduce sparsity in the dictionary and estimation process to propose an efficient algorithm for volume fraction and fiber orientation estimation. The positivity and sum-to-one constraints of volume fractions make the sparse representation and inference especially difficult. We fix the sparsity level (maximum number of fiber orientations to be considered) to a small number (n_0 , $n_0 \ll N$). The problem is then formulated as a linear un-mixing inference where the diffusion signals correspond to a mixture of the dictionary components with positive weights \mathbf{f} . We follow a semi-supervised hierarchical Bayesian linear un-mixing approach [12] for sparsity-based inference of fibers. The method is semi-supervised because the dictionary is known for a given diffusivity, gradient directions, b-values, and possible orientations, but we do not know either the fiber orientations or the volume fractions within each compartment.

The likelihood function of the HR data can be expressed by (6)

$$p(y_{HR} | f, \sigma^2) = \left(\frac{1}{2\pi\sigma^2} \right)^{\frac{K}{2}} e^{-\frac{\|y_{HR} - Ef\|_2^2}{2\sigma^2}} \quad (6)$$

where σ^2 corresponds to the variance of the error in representation of y_{HR} by using dictionary \mathbf{E} and volume fractions \mathbf{f} . Let $f^+ = [f_1, \dots, f_N]^T$ be the volume fractions of the anisotropic compartments, then f^+ belongs to a simplex S (7).

$$S = \left\{ f^+ | f_n \geq 0, \forall n=1, \dots, N, \sum_{n=1}^N f_n \leq 1 \right\} \quad (7)$$

A sparsity-promoting prior (section 2.4) is used for the anisotropic volume fractions. The volume fractions posterior is given by (8) [8, 12].

$$p(f^+ | y_{HR}, \sigma^2) \sim e^{-(f^+ - \mu_f)^T \Lambda_f^{-1} (f^+ - \mu_f)} 1_S(f^+) \quad (8)$$

where

$$\Lambda_f = \left[\sigma^{-2} \left(E_{n0}^+ - e_0 u^T \right)^T \left(E_{n0}^+ - e_0 u^T \right) \right]^{-1}, \quad (9)$$

$$\mu_f = \sigma^{-2} \Lambda_f \left(E_{n0}^+ - e_0 u^T \right)^T (y_{HR} - e_0), \quad (10)$$

with $u = [1, \dots, 1]^T$. E_{n0}^+ contains the columns of E that correspond to the $n0$ non-zero coefficients in f^* (effective dictionary) and e_0 is the column corresponding to the isotropic compartment (*ball*). $1_S(f^+)$ is one if $f^* \in S$ and zero otherwise.

The posterior of σ^2 given the data and sparse representation is given by the inverse Gamma (IG) distribution (11) [12]

$$p(\sigma^2 | y_{HR}, f) \sim IG(K/2, \|y_{HR} - Ef\|^2/2). \quad (11)$$

The generation of samples according to (8–10) is accomplished using a Gibbs sampler, where a column in the effective dictionary E_{n0}^+ can be switched at random with another to test a different fiber orientation.

2.4 Priors

We utilized a sparsity promoting prior for the volume fractions estimation. The prior utilized is a dirichlet prior (12) [13] which depends on the data.

$$p(f_n) = \prod_{n=1}^N f_n^{\phi-1}, \phi < 1 \quad (12)$$

When the hyper-parameter ϕ is small ($\phi < 1$), the prior takes a larger value as the number of volume fractions whose values are close to zero increases, which is desirable for enforcing sparsity.

We followed the rest of the parameter priors and inference procedure as in RubiX [1]. The priors used for S^0 and σ are unconditional and non-informative (uniform). Conditional priors are used for orientation and diffusivity and are defined as a mixture of Watson distributions with non-informative hyper-parameter for orientation and normal distribution with informative hyper-parameter for diffusivity.

3 Experiments and Results

3.1 Simulated Data

Synthetic data is simulated using Camino [14] (Diffusion Tensor-Cylinder-Sphere model) to have the ground truth for comparison of estimated fiber orientations. Single and crossing fiber structures (with 2 and 3 fibers) with image size $10 \times 10 \times 2$ (LR) and $20 \times 20 \times 4$ (HR) are simulated. The orientations of fibers at each LR voxel are randomly selected. Diffusion signals are simulated along 133 uniformly distributed directions. The noise free HR signal is created by expanding the LR image size to HR image size along all three coordinates without partial voluming. Rician noise is added to both LR and HR images by adding zero-mean Gaussian signal in quadrature. A factor of $8/\sqrt{2}$ is maintained [1] in the ratio of SNR of LR to that of HR signal (lesser noise in LR data). Data with two SNRs, 15 and 25, are simulated. Under-sampling of diffusion directions is done by a factor of up to 4 to simulate acceleration in image acquisition.

The algorithm performance is compared with the ball & stick model applied to the HR dataset (using *bedpostX* tool [4] in FSL) and RubiX [1] applied to HR and LR datasets. Both RubiX and the proposed method are applied to HR and LR datasets, with the first 67 measurements forming the *no-acceleration* data. This is done in order to match the acquisition time, making the comparisons fair. The 67 measurements are under-sampled again up to a factor of 4 to simulate accelerations. For under-sampling we used the protocol proposed by Caruyer *et al.* [15], which makes any first N samples isotropic. Fig. 1 shows the error in orientation estimation and its variation with acceleration. On comparison, the proposed sparse approach provided better accuracy in estimation. The variation in accuracy with acceleration is less in the proposed approach. Fig. 2 (a) shows mean span of the 95% cones of orientational uncertainty, which is a measure of the width of estimated distribution, representing the uncertainty in estimation. On comparison, the proposed method yielded lower estimation uncertainty.

3.2 In-Vivo MRI data

We acquired in-vivo dMRI data from a healthy subject using a 3T Siemens Prisma scanner. For HR acquisitions the acquisition matrix was $140 \times 140 \times 92$ voxels with a resolution of $1.5 \times 1.5 \times 1.5 \text{ mm}^3$. For LR acquisitions the resolution was reduced to $3 \times 3 \times 3 \text{ mm}^3$ for an acquisition matrix size $70 \times 70 \times 46$ voxels. Diffusion weighting was applied in 200 evenly spaced directions with a b-value of 1500 s/mm^2 . Twenty one volumes without diffusion weighting are equally interleaved in the dataset.

Fig. 2 (b) shows a representative comparison of fiber orientation estimates from Corpus Callosum area, demonstrating the invariance in estimates with acceleration. In addition we analyzed several regions of interest (ROIs) in the brain and found that the proposed method resolved more number of fiber crossings at a lesser uncertainty. Included result (Fig.3) is the number of two and three fiber crossings from left/right superior longitudinal fasciculus (SLF) and left/right posterior corona radiata (PCR). It can be noticed that, while RubiX tends to recover fewer second and third fiber crossings as under-sampling factor increases,

the proposed method performs equally well even with only a quarter of the original diffusion gradients.

4 Conclusions

Reducing acquisition time and maintaining SNR are two challenging goals in dMRI acquisition. We proposed a processing method to achieve these goals simultaneously, extending and improving an existing multi-resolution approach (RubiX) by introducing sparsity. The proposed sparse Bayesian algorithm is useful in reconstructing fiber orientations from accelerated (under-sampled) dMRI data. The algorithm provided better estimation accuracy at lower uncertainty. The near linear behavior of the estimation error and the number of detected fiber crossings with acceleration shows the utility of the proposed approach.

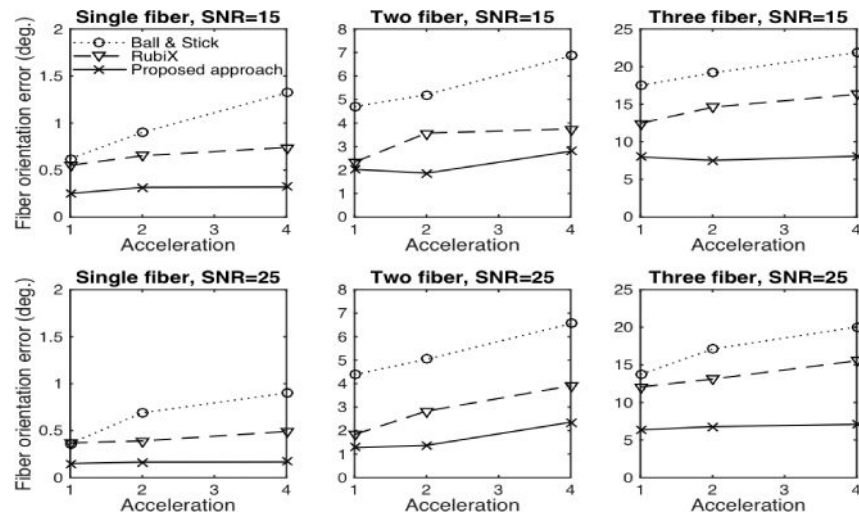
Acknowledgments

This work was partly supported by NIH grants P41 EB015894, P30 NS076408, R01 EB008432, and the Human Connectome Project (U54 MH091657).

References

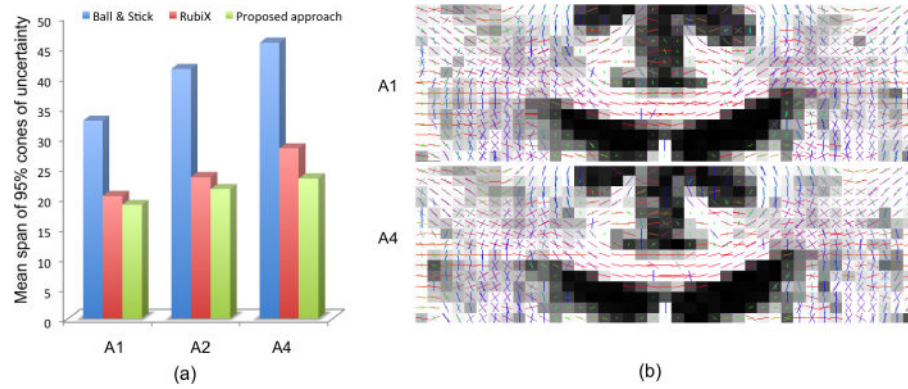
1. Sotiropoulos SN, Jbabdi S, Andersson JL, Woolrich MW, Ugurbil K, Behrens TEJ. Rubix: Combining spatial resolutions for bayesian inference of crossing fibers in diffusion mri. *Ieee Trans Med Imag*. 2013; 32:969–982.
2. Behrens TE, Woolrich MW, Jenkinson M, Johansen-Berg H, Nunes RG, Clare S, Matthews PM, et al. Characterization and propagation of uncertainty in diffusion-weighted mr imaging. *Magn Reson Med*. 2003; 50:1077–1088. [PubMed: 14587019]
3. Panagiotaki E, Schneider T, Siow B, Hall MG, Lythgoe MF, Alexander DC. Compartment models of the diffusion mr signal in brain white matter: A taxonomy and comparison. *NeuroImage*. 2012; 59:2241–2254. [PubMed: 22001791]
4. Behrens TE, Berg HJ, Jbabdi S, et al. Probabilistic diffusion tractography with multiple fibre orientations: What can we gain? *Neuroimage*. 2007; 34:144–155. [PubMed: 17070705]
5. Ugurbil K, et al. Pushing spatial and temporal resolution for functional and diffusion mri in the human connectome project. *Neuroimage*. 2013; 80:80–104. [PubMed: 23702417]
6. Sotiropoulos SN, Jbabdi S, Xu J, Andersson JL, Moeller S, et al. Advances in diffusion mri acquisition and processing in the human connectome project. *Neuroimage*. 2013; 80:125–143. [PubMed: 23702418]
7. Scherrer B, Gholipour A, Warfield SK. Super-resolution reconstruction to increase the spatial resolution of diffusion weighted images from orthogonal anisotropic acquisitions. *Medical image analysis*. 2012; 16:1465–1476. [PubMed: 22770597]
8. Tipping ME. Sparse bayesian learning and the relevance vector machine. *Journal of Machine Learning Research*. 2001; 1:211–244.
9. Ji S, Dunson D, Carin L. Multitask compressive sensing. *Ieee Transactions on Signal Processing*. 2009; 57:92–106.
10. Otazo R, Cande's E, Sodickson DK. Low-rank plus sparse matrix decomposition for accelerated dynamic mri with separation of background and dynamic components. *Magnetic Resonance in Medicine*. 2015; 73:1125–1136. [PubMed: 24760724]
11. Paquette M, Merlet S, Gilbert G, Deriche R, Descoteaux M. Comparison of sampling strategies and sparsifying transforms to improve compressed sensing diffusion spectrum imaging. *Magnetic Resonance in Medicine*. 2015; 73:401–416. [PubMed: 24478106]

12. Dobigeon N, Tourneret JY, Chang CI. Semi-supervised linear spectral un-mixing using a hierarchical bayesian model for hyperspectral imagery. *Ieee Transactions on Signal Processing*. 2008; 56:2684–2695.
13. Araki S, Nakatani T, Sawada H, Makino S. *Ieee: Blind sparse source separation for unknown number of sources using gaussian mixture model fitting with dirichlet prior. IEEE ICASSP Proceedings*. 2009:33–36.
14. Cook, PA., Bai, Y., Nedjati-Gilani, S., Seunarine, KK., Hall, MG., Parker, GJ., C, AD. Scientific Meeting of ISMRM. Seattle, WA, USA: 2006. Camino: Open-source diffusion-mri reconstruction and processing.
15. Caruyer E, Cheng J, Lenglet C, Sapiro G, Jiang T, Deriche R. Optimal design of multiple q-shells experiments for diffusion mri. *MICCAI Workshop Comput Diffusion MRI (CDMRI)*. 2011

**Fig. 1.**

Comparison of fiber orientation estimation error and its variation with acceleration.

Acceleration of 1, 2 and 4 represent the cases of no-acceleration, acceleration by a factor of 50% and that by a factor of 75% respectively. Y-axis represents mean error in 2 and 3 fiber cases.

**Fig. 2.**

(a) Mean span of 95% cones of uncertainty (representative simulation case, 2 fiber, SNR 15),
 (b) Comparison showing the stability of fiber orientation estimates with acceleration (in-vivo data, overlapped on sum of anisotropic volume fractions). A1–A4 represent accelerations up to 4.

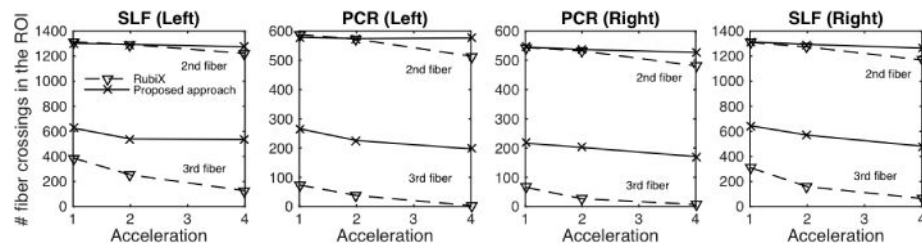


Fig. 3.

Variation in number of second and third fiber crossings (with volume fraction greater than 5%) in four ROIs, left/right superior longitudinal fasciculus (SLF) and left/right posterior corona radiata (PCR).